Estuarine, Coastal and Shelf Science 88 (2010) 350–356

Contents lists available at ScienceDirect

Estuarine, Coastal and Shelf Science

journal homepage: www.elsevier.com/locate/ecss

Characteristics of chromophoric dissolved organic matter in the nearshore waters of the western Taiwan Strait

Cuifen Du [a], Shaoling Shang [a,*], Qiang Dong [a], Chuanmin Hu [b], Jingyu Wu [a]

[a] State Key Laboratory of Marine Environmental Science, Xiamen University, Xiamen 361005, Fujian, China
[b] College of Marine Science, University of South Florida, 140 Seventh Ave. S., St. Petersburg, FL 33701, USA

ARTICLE INFO

Article history:
Received 9 November 2009
Accepted 23 April 2010
Available online 5 May 2010

Keywords:
CDOM
absorption coefficient
fluorescence
remote sensing
coastal waters
Western Taiwan Strait

ABSTRACT

Absorption and fluorescence of chromophoric dissolved organic matter (CDOM) in the nearshore waters of the western Taiwan Strait were examined in April and October of 2008. CDOM absorption coefficient at 412 nm ($a_g(412)$ in m^{-1}) showed an inversed linear relationship with salinity, indicating conservative mixing between freshwater and seawater, although the relationship changed with seasons and locations. On average, except in the vicinity of two major rivers (Minjiang River and Jiulongjiang River), $a_g(412)$ was higher in October (dry season) (0.173 ± 0.036 m^{-1}) than in April (wet season) (0.123 ± 0.059 m^{-1}). This observation is counter intuitive but consistent with those derived from MODIS satellite measurements. Combined with the CDOM EEM spectra (fluorescence excitation–emission matrix), the results suggest that 1) Minjiang River and Jiulongjiang River were the primary land-based CDOM sources; 2) The marine end-members were controlled by the South China Sea Warm Current in April and the Zhe-Min Coastal Water in October; 3) The land-based CDOM was more from sewage than from soil leaching; and 4) Light absorption in the blue wavelengths was dominated by CDOM and detritus.

1. Introduction

Chromophoric dissolved organic matter (CDOM), an optically active component of DOM, plays an important role in carbon cycling (Coble, 2007). CDOM provides an effective sun shade, modulates the underwater light field and thus affects growth of phytoplankton and other aquatic organisms (e.g. Jerlov, 1968; Karentz and Lutze, 1990). Therefore, it is critical to study the abundance, sources, compositions, and the final fates of CDOM at local and global scales to eventually model and forecast variations of CDOM as well as carbon budgets globally (e.g. Mannino et al., 2008).

While global scale CDOM distributions can only be assessed through satellite remote sensing (e.g., Siegel et al., 2002), at the local scale, field surveys are often required. Several studies showed relatively low abundance of CDOM in estuaries of China (Zhu and Li, 2003; Chen et al., 2004, 2007; Hong et al., 2005; Guo et al., 2007). Yet CDOM characteristics in the broad coastal regions of China, where heavy and rapid industrialization and urbanization occurred in the past decades, are still unclear. Obviously, targeted sampling and studies are required for all coastal regions of China. Such studies will not only put the urbanization-heavy Chinese coastal waters in the global perspective, but also provide baseline information to evaluate potential impact of climate change and anthropogenic activities.

The Taiwan Strait is a shallow channel connecting the East China Sea (ECS) to the South China Sea (SCS). Warm, saline, and oligotrophic water enters the Taiwan Strait from the SCS as the SCS Warm Current (SCSWC) while cold, fresh, and eutrophic water intrudes from the ECS as the Zhe-Min Coastal Water (ZMCW). The northeast monsoon in the winter drives the ZMCW towards the south and the southwest monsoon in the summer favors the input from the south (e.g. Jan et al., 2002; Hong et al., 2009). Several medium-sized rivers (e.g., Minjiang, Jinjiang and Jiulongjiang Rivers; the annual mean runoff are 621×10^8 m^3, 51.3×10^8 m^3 and 117×10^8 m^3, respectively) and small streams are located on the western coast (mainland China) of the strait. This is where the impact of the rapid industrialization on the coastal-water quality has been of great concern (http://www.fjepb.gov.cn). However, CDOM characteristics in this biologically and economically important region have never been reported. Here, using data collected from two field surveys in combination with remote sensing data, we report our preliminary findings on the CDOM spatial-temporal distributions, dynamics, and its potential origin. And we also evaluate the role of CDOM in the water-column light absorption.

* Corresponding author.
E-mail address: slshang@gmail.com (S. Shang).

0272-7714/$ – see front matter © 2010 Elsevier Ltd. All rights reserved.
doi:10.1016/j.ecss.2010.04.014

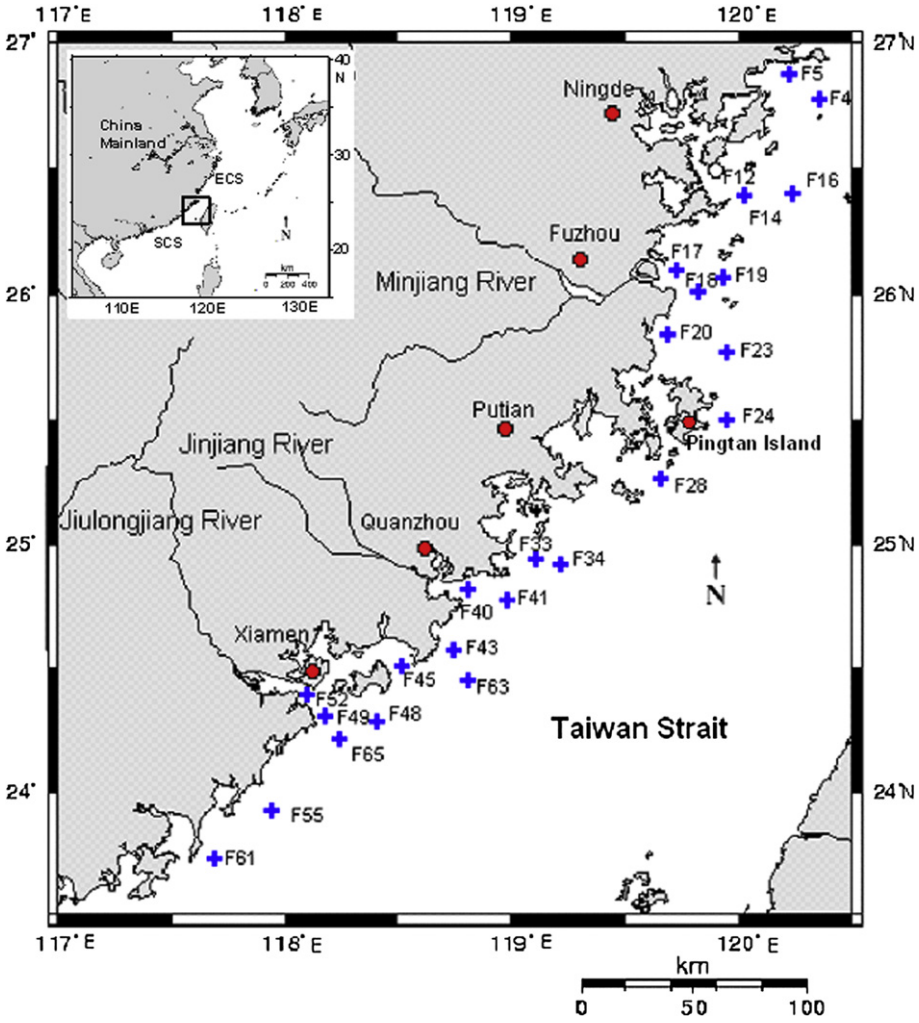

Fig. 1. Location of sampling stations in the nearshore waters of western Taiwan Strait.

2. Methods

2.1. Sample collection and measurements

Samples were collected from surface waters during two cruises on the R/V Yanping-II from 12 to 16 April 2008 and from 29 October to 1 November 2008 (Fig. 1). The entire procedure was performed according to the Ocean Optics Protocols Version 2.0 (Mitchell et al., 2000), while measurements of CDOM fluorescence excitation–emission matrix (EEM) spectra followed Coble et al. (1998). The methods were detailed in a previous study in the Pearl River Estuary (Hong et al., 2005), but modified slightly in this study.

First, a nonlinear least square regression between 400 and 500 nm was used to obtain the magnitude (at 412 nm, to facilitate comparison with remote sensing data) and spectral slope (S, in nm^{-1}) of CDOM absorption.

Second, particulate absorption was measured with a dual-beam PE Lambda 950 spectrophotometer equipped with an integrating sphere. Because the samples were collected nearshore, instead of the T method recommended in the NASA protocol (Mitchell et al., 2000), a modified Transmittance–Reflectance (T–R) method was adopted (Dong et al., 2008). This was based on Tassan and Ferrari's approach proposed in 2002. The pathlength amplification effect (β) was derived from local samples (Dong et al., 2008): $\beta^{-1} = (0.135 + 0.225 \times OD(\lambda)) \times \lambda^{0.203}$, where OD refers to the optical density.

Third, phytoplankton absorption coefficients (a_{ph}) were obtained using methanol extraction. For the April samples, because of a methanol contamination, absorption coefficients of the non-algal particles (a_d) and a_{ph} were modeled following Bricaud and

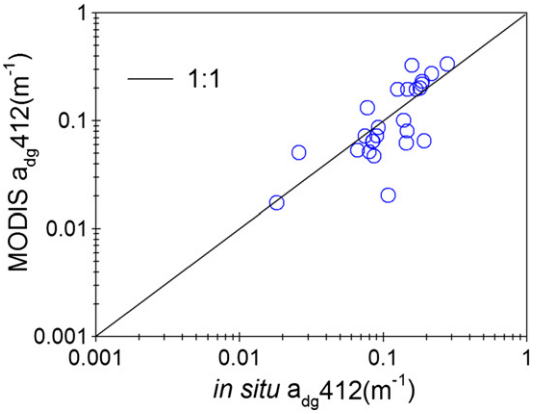

Fig. 2. Field measured $a_{dg}(412)$ versus concurrent MODIS remote sensing reflectance derived $a_{dg}(412)$ by using QAA.

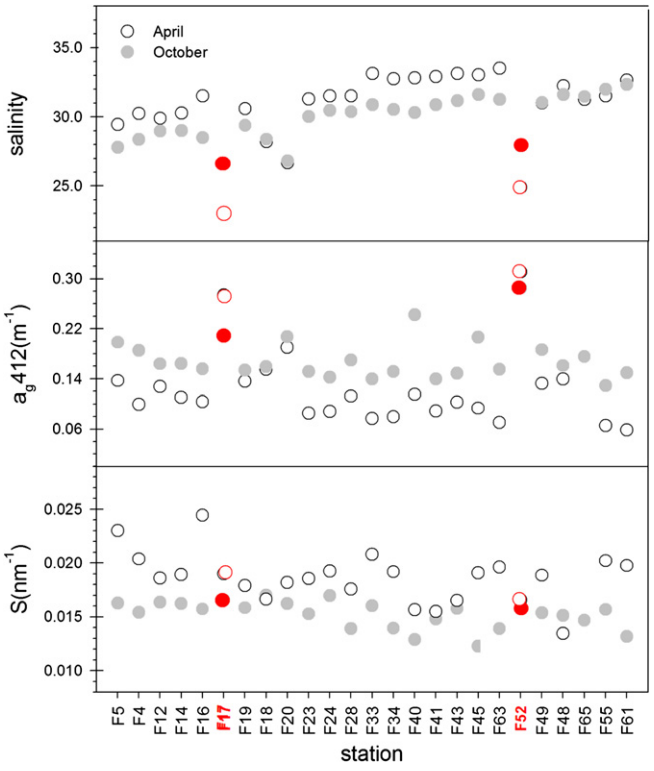

Fig. 3. Variations of salinity and $a_g(412)$. Empty symbols show data for April, and filled symbols are for October. Red symbols annotate the two stations located out of the MR mouth (F17) and the JR mouth (F52).

Stramski (1990), but $r_1 = a_{ph}(505)/a_{ph}(380)$ and $r_2 = a_{ph}(580)/a_{ph}(692.5)$ were adjusted to 0.61 and 0.86 according to the a_{ph} measurements in October.

Surface chlorophyll-*a* concentrations (Chl *a* in mg/m^3) were measured using the fluorometric method (Parsons et al., 1984). And an underway system (Seabird (SBE21) thermosalinograph) was used to record surface temperature (in °C) and salinity (in Practical Salinity Scale) continuously.

2.2. MODIS data processing

Remote sensing reflectance (R_{rs} in sr^{-1}) was derived from the Moderate Resolution Imaging Spectroradiometer (MODIS) measurements during 2003–2008. These daily 1-km resolution data were obtained from the U.S. NASA Distributed Active Archive Center (DAAC). The absorption coefficient of CDOM and non-algal particles (a_{dg}) was then derived from MODIS $R_{rs}(\lambda)$ using a quasi-analytical bio-optical inversion algorithm (QAA V5) originally designed for optically deep waters (Lee et al., 2002; Lee et al., 2009). It is applicable to our study region since the light penetration depth estimated from *in situ* optical data and the Lee (2005) model is shallower than the physical depth. Because of the similarity between the spectral shapes of CDOM and non-algal particles (Lee et al., 2002), it is currently impossible to further partition a_{dg} into a_g and a_d (here a_d includes contributions from both organic detrital particles and inorganic suspended sediments).

The MODIS a_{dg} data generally agreed with those determined from concurrent *in situ* samples (Fig. 2, RMS error in log scale = 0.241 for $a_{dg}(412)$ between 0.02 and 0.28 m^{-1}, $n = 25$, $R^2 = 0.60$). Due to frequent cloud cover, daily data in April and

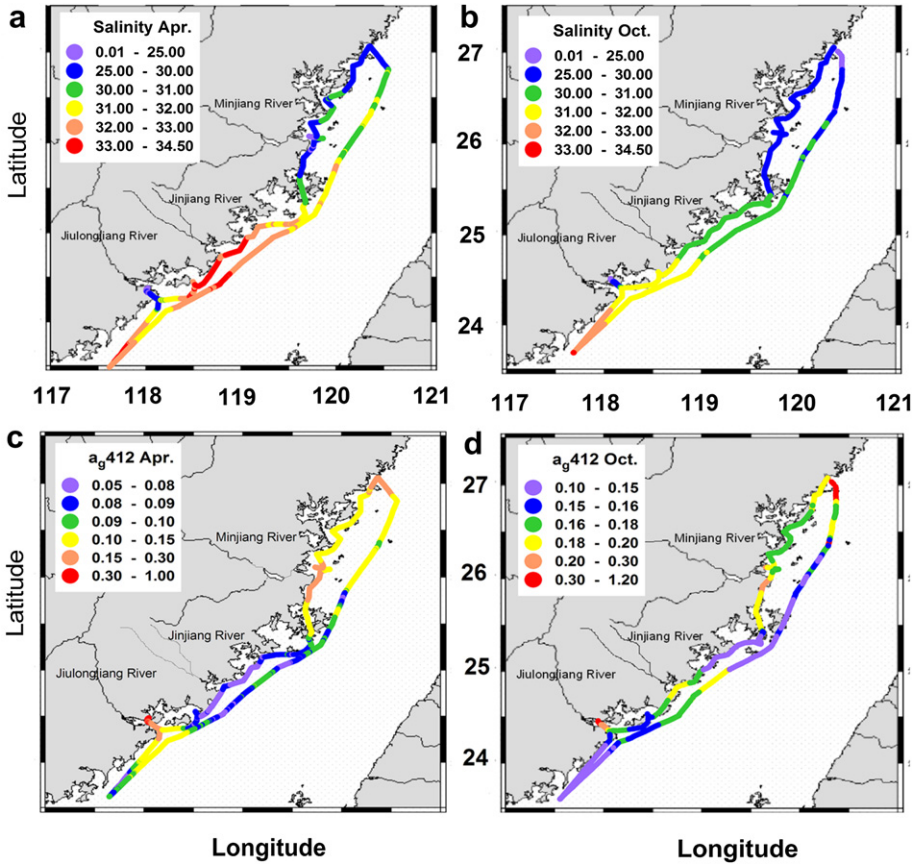

Fig. 4. Salinity and $a_g(412)$ along the ship track for April (a and c) and October (b and d). Salinity was measured continuously through an underway system, and $a_g(412)$ was estimated based on the observed salinity and the relationship between $a_g(412)$ and salinity.

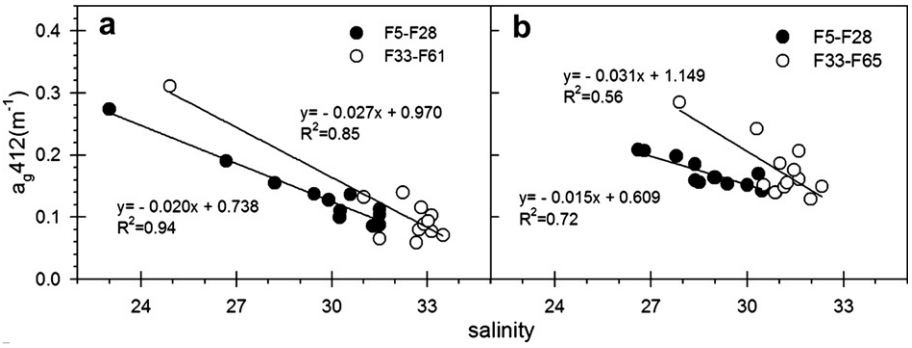

Fig. 5. The relationship between $a_g(412)$ and salinity for April (a) and October (b). Empty circles are for the stations located in the north section near the MR mouth, while solid circles are for the stations located in the south section near the JR mouth.

October in 2003–2008 were averaged to produce climatological monthly means.

3. Spatial-temporal variations of $a_g(412)$

The spatial heterogeneity in both $a_g(412)$ and salinity is apparent (Fig. 3). In April, relatively high $a_g(412)$ (>0.18 m^{-1}) and low salinity (<27) were found at three stations (F17, F20, F52) in the vicinity of Minjiang River estuary (MRE) and Jiulongjiang River estuary (JRE). The minimum $a_g(412)$ was south of the JRE, adjacent to the SCS. In October, relatively high $a_g(412)$ (>0.20 m^{-1}) was found at the same three stations as in April, and at two other stations (F40 and F45). The latter two stations are adjacent to the two heavily industrialized cities in Fujian (Xiamen and Quanzhou), and therefore may have received substantial terrestrial CDOM-rich discharges.

The cruise stations were partitioned into two groups depending on their proximity to the two estuaries (MRE and JRE), and by following the previous oceanographic zoning of the northern and the southern Taiwan Strait (i.e. use the Pingtan Island as a boundary, Zeng and Hong, 1980): the north section (F4–F28) and the south section (F33–F65). Fig. 5 shows that such a partition resulted in inversed linear relationship between $a_g(412)$ and salinity for both sections in both seasons, indicating conservative mixing for low salinity water (<30). These linear relationships were then used to derive continuous $a_g(412)$ along the ship tracks from the underway surface salinity (Fig. 4).

Near the two main river mouths (F17 and F52), $a_g(412)$ was higher in April than in October (Fig. 3), while opposite patterns were observed away from the two estuaries. In general, the spatial gradient and dynamic range of $a_g(412)$ were lower in October (0.13–0.28 m^{-1}, variance = 20.2%) than in April (0.06–0.31 m^{-1}, variance = 48.3%); while the areal mean $a_g(412)$ of the sampling region was higher in October than in April (0.173 ± 0.036 m^{-1} versus 0.123 ± 0.059 m^{-1}). Similar patterns were obtained when $a_{dg}(412)$ was considered (0.320 ± 0.097 m^{-1} in October versus 0.256 ± 0.134 m^{-1} in April), where a significant contribution (50%) resulted from $a_d(412)$.

The MODIS climatological monthly mean $a_{dg}(412)$ for April and October also showed higher $a_{dg}(412)$ in October (Fig. 6), which was consistent with *in situ* measurements above. Indeed, for the near-shore waters (<30 m depth) where the *in situ* stations are located, MODIS $a_{dg}(412)$ was 0.33 ± 0.19 m^{-1} in October and 0.23 ± 0.14 m^{-1} in April, nearly identical to those from field measurements.

Corresponding to the April/October difference in $a_g(412)$, higher spectral slope (S) values were found in April (0.0187 ± 0.0023 nm^{-1}, 0.0134–0.0245 nm^{-1}) than in October (0.0153 ± 0.0013 nm^{-1}, 0.0123–0.0170 nm^{-1}). This is typical for coastal regions where high-CDOM waters are often associated with lower S values, indicating terrestrial origin. For example, in Chesapeake Bay, S (280–650 nm) varied between 0.015 and 0.025 nm^{-1}, with low slope values associated with low salinity and high CDOM absorption (Rochelle-Newall and Fisher, 2002).

4. CDOM dynamics and origin

The Minjiang River (MR) freshwater discharge from April to September (wet season) accounts for ~74% of the annual runoff (Table 1, (Zhang, 2000)). Because of the watershed similarity and location proximity, Jiulongjiang River (JR) discharge is believed to have similar seasonality. Thus, in stations close to the two river

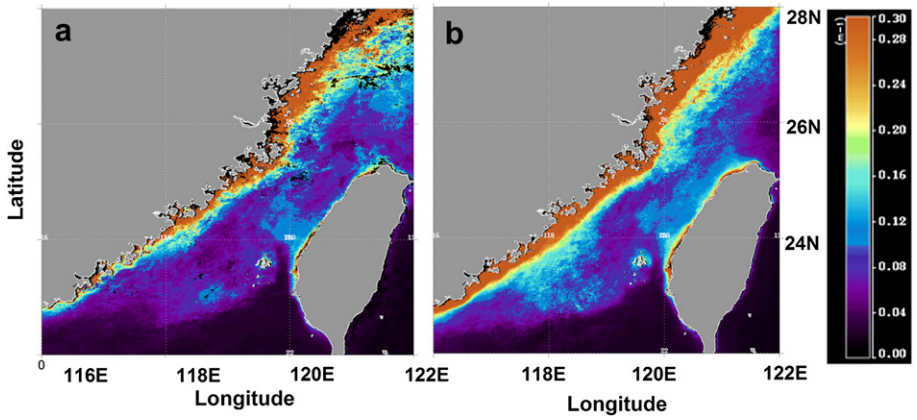

Fig. 6. The distribution of climatological monthly mean $a_{dg}(412)$ derived from MODIS observations for April (a) and October (b).

Table 1
Monthly rainfall and flow of the Minjiang River recorded at Zhuqi.[a]

	Jan.	Feb.	Mar.	Apr.	May	Jun.	Jul.	Aug.	Sep.	Oct.	Nov.	Dec.	(Apr.-Sep.)
Rainfall (mm)	49.5	83.9	134.6	154.2	220.9	224.5	139.4	175.5	161.6	47.8	37.7	34.5	1076.1
% of annual Value	3.4	5.7	9.2	10.5	15.1	15.3	9.5	12	11	3.3	2.6	2.4	73.4
Runoff (10^8 m^3)	16.6	22.9	45.2	62.6	91.8	115.3	59.6	40.4	32.8	23.3	17.7	16.2	577.3
% of annual Value	3.1	4.2	8.3	11.5	16.9	21.2	10.9	7.4	6	4.3	3.2	3	73.9

[a] Zhang, 2000.

mouths, higher $a_g(412)$ was observed in April than in October. Away from the two estuaries, higher $a_g(412)$ was found in October, suggesting other CDOM sources. The ZMCW originates from the mixing of alongshore runoff and seawater from the ECS (Wu, 1982), and thus is relatively richer in CDOM than the SCSWC. The ZMCW is more pronounced in the western Taiwan Strait from September to February (e.g. Wang and Chen, 1989), therefore may be responsible for the higher $a_g(412)$ in October. This possibility is also supported by the lower salinity in October (Figs. 3 and 4).

The same mechanism could also explain why the north section showed higher $a_g(412)$ than the south section. JR runs by Xiamen, one of the two most heavily industrialized cities in Fujian, carrying more pollutants than MR and leading to higher $a_g(412)$ at the JR mouth (F52) than at the MR mouth (F17). However, because the marine end member (i.e. SCSWC) had low $a_g(412)$, relatively lower $a_g(412)$ was observed in the south section. Opposite situation occurred in the north section, where low riverine $a_g(412)$ end member (MR) was mixed with high $a_g(412)$ marine end member (ZMCW)). For the same reasons, higher spatial variability of $a_g(412)$ and higher S values were found in April than in October.

The high correlation between $a_g(412)$ and salinity (Fig. 5, $R^2 = 0.94$ and 0.85 (April) and 0.72 and 0.56 (October) for the north and the south sections, respectively) suggested terrestrial CDOM origin. Extrapolation to salinity = 0 inferred freshwater end members with $a_g(412)$ 0.74 m^{-1} and 0.97 m^{-1} (April), and $a_g(412)$ 0.61 m^{-1} and 1.15 m^{-1} (October) for the north and south sections, respectively. Using a mean slope $S = 0.0169$ nm^{-1}, $a_g(355)$ at zero salinity in the south section was estimated to be 2.54 m^{-1} in April and 3.01 m^{-1} in October. This is opposite from the results of Guo et al. (2007) ($a_g(355)$ 3.2 m^{-1} in April and 2.2 m^{-1} in October in the JRE), possibly due to the multiple river/stream CDOM sources to the entire south section. However, such a scenario of higher freshwater CDOM in the dry season (October) than in the wet season (April) is counter intuitive. This implied that freshwater CDOM did not primarily originate from soil leaching. To verify this hypothesis, CDOM EEMs were analyzed.

Three distinct principal fluorophore types were detected from the October EEMs samples: tryptophan-like (T, EX/EM_{max}: 230/350), UV humic-like (A, EX/EM_{max}: 250/450), and visible-terrestrial humic-like (C, EX/EM_{max}: 325/426) fluorophores (Fig. 7). The fluorescence intensity at Station F61 (southern end of the study region, partially representing SCSWC) was much weaker than at Station F5 (northern end of the study region, partially representing ZMCW). Similar to the observations in the Pearl River estuary (Hong et al., 2005) but in contrast to those observed in other estuaries (e.g. Del Castillo et al., 1999), T fluorophores showed the strongest signals among all fluorophores for all samples. The fluorescence intensity ratio of T to C ranged between 1.8 and 5.3, with lower average values (2.7 ± 0.5) for the north section than for the south section (3.2 ± 0.9).

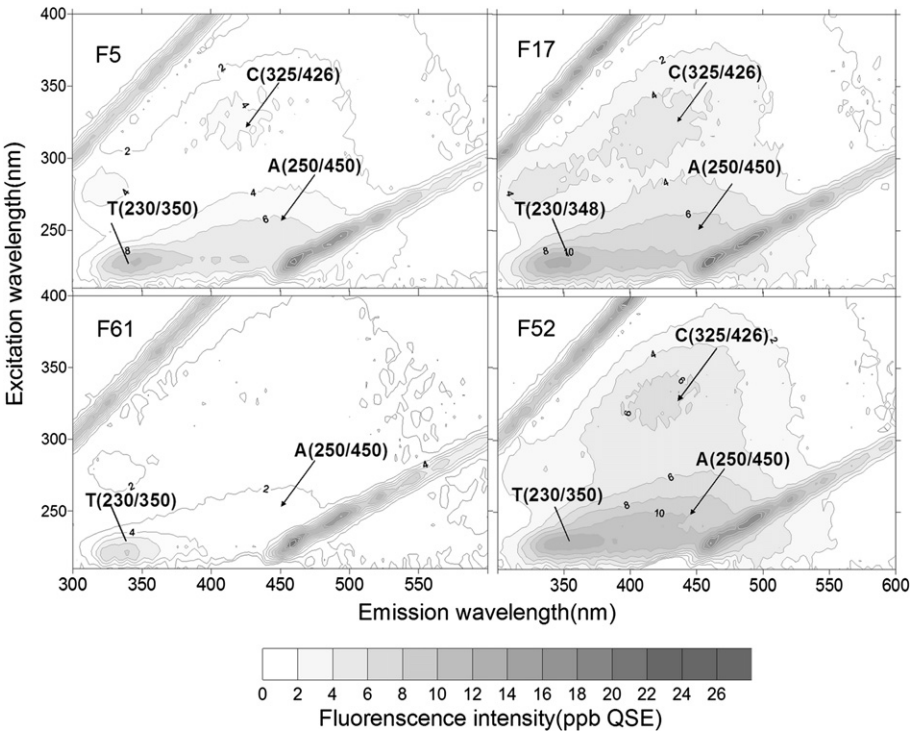

Fig. 7. Contour plot of the fluorescence matrices at Station F5, F61, F17, F52 in October 2008.

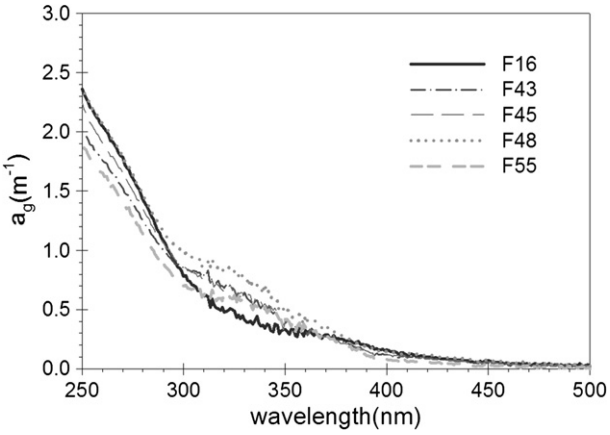

Fig. 8. CDOM absorption spectra with local peaks between 300 and 400 nm from some April samples, suggesting the existence of MAAs that are released by phytoplankton and/or zooplankton.

The dominant T signal suggested that the CDOM resulted primarily from sewage, with fluorescence properties similar to animal farm wastes (Baker, 2002). Terrestrial humic or fulvic substances produced from decayed plant matter leaching from soils were minor. Thus, assuming sewage is relatively stable over time, less precipitation in October would lead to higher freshwater CDOM. Furthermore, weak fluorescence intensity at Station F61, as compared to Station F5, clearly showed the differences in CDOM components between the SCSWC and the ZMCW. Likewise, different T/C ratios from the two sections indicated different land-based CDOM components. The latter would explain why the north section did not show similar April/October differences in the freshwater end member of $a_g(412)$.

Aside from the terrestrial CDOM source, local CDOM production might not be ignored. CDOM could be produced from bacterial degradation of organic matters originated from algal cells (e.g. Hu et al., 2006). Although there was no correlation between Chl *a* and $a_g(412)$, a CDOM absorption peak between ~300 and 360 nm from some April samples (Fig. 8) suggested the likely existence of MAAs (mycosporine- like amino acids), which were released by phytoplankton and/or zooplankton (e.g. Whitehead and Vernet, 2000). However, such contributions to the CDOM pool are believed to be minor, as compared with those from terrestrial runoff.

5. Implications for ocean color remote sensing

In CDOM-rich waters, it is difficult to derive accurate Chl *a* estimates from ocean color satellite measurements because both CDOM and phytoplankton strongly absorb blue light and CDOM may be erroneously interpreted as phytoplankton (e.g. Carder et al., 1989). Thus, it is desirable to evaluate the relative contributions of CDOM and phytoplankton to blue light (443 nm) in this coastal region.

Our results of $a_{dg}(443)/a_{ph}(443)$ showed substantial variability in both space and time, ranging from 0.68 to 7.25 (2.57 ± 1.63) in April and 1.22 to 5.99 (3.94 ± 1.45) in October. More than 50% of the 31 samples showed ratios >3.0. This may result in difficulties in accurate Chl *a* retrievals from satellite measurements. Indeed, the climatological monthly mean MODIS Chl *a* (OC3 algorithm, O'Reilly et al., 2000) at the sampling stations was 3.25 mg m^{-3} in April and 3.53 mg m^{-3} in October, significantly different from the in situ values (2.40 mg m^{-3} and 1.56 mg m^{-3} for April and October, respectively). More work is required to derive reliable MODIS Chl *a* using alternative approaches, for example from solar stimulated fluorescence (Hu et al., 2005).

6. Conclusion

The study here, based on two field surveys and MODIS remote sensing data, provides a preliminary view of CDOM characteristics as well as its origin and controlling mechanisms in the nearshore waters of the western Taiwan Strait. The most striking result is that higher CDOM absorption was found in the dry season than in the wet season. Although this observation is counter intuitive, it can be well explained by local CDOM sources and ocean circulations. Given the continuous urbanization in the nearby coastal area, it is desirable to conduct routine surveys and develop dynamic models to assess CDOM's origin, fate, and long-term changes in this economically and ecologically important coastal water.

Acknowledgements

This work was supported by the High-Tech R & D Program of China (#2006AA09A302 & 2008AA09Z108), the China Scholarship Council, the NSF-China (#40821063), the Program of Introducing Talents of Discipline to Universities (#B07034), and the U.S. NASA (NNX09AT50G). We are thankful to the Environmental Protection Agency of Xiamen, Prof. J.Y. Hu and Mr. Q. L. Pi of Xiamen University, and the crew of the R/V Yanping II, for their help in collecting *in situ* data. We also thank three anonymous reviewers and the editor for their critical comments.

References

Baker, A., 2002. Fluorescence excitation emission matrix characterization of river waters impacted by a Tissue Mill effluent. Environmental Science and Technology 36, 1377–1382.
Bricaud, A., Stramski, D., 1990. Spectral absorption coefficients of living phytoplankton and nonalgal biogenous matter: a comparison between the Peru upwelling area and the Sargasso Sea. Limnology and Oceanography 35, 562–582.
Carder, K.L., Steward, R., Harvey, G., Ortner, P., 1989. Marine humic and fulvic acids: their effects on remote sensing of ocean chlorophyll. Limnology and Oceanography 34, 68–81.
Chen, Z., Li, Y., Pan, J., 2004. Distributions of colored dissolved organic matter and dissolved organic carbon in the Pearl River Estuary, China. Continental Shelf Research 24, 1845–1856.
Chen, Z., Hu, C., Conmy, R.N., Muller-Karger, F., Swarzenski, P., 2007. Colored dissolved organic matter in Tampa Bay, Florida. Marine Chemistry 104, 98–109.
Coble, P.G., Castillo, C.E.D., Avril, B., 1998. Distribution and optical properties of CDOM in the Arabian Sea during the 1995 Southwest Monsoon. Deep-Sea Research 45, 2195–2223.
Coble, P.G., 2007. Marine optical biogeochemistry: the chemistry of ocean color. Chemical Reviews 107, 402–418.
Del Castillo, C.E., Coble, P.G., Morell, J.M., Lopez, J.M., Corredor, J.E., 1999. Analysis of the optical properties of the Orinoco River plume by absorption and fluorescence spectroscopy. Marine Chemistry 66, 35–51.
Dong, Q., Hong, H., Shang, S., 2008. A new approach to correct for pathlength amplification in measurements of particulate spectral absorption by the quantitative filter technique. Journal of Xiamen University (Natural Science) 47, 556–561 (in Chinese, with English Abstr).
Guo, W., Stedmon, C.A., Han, Y., Wu, F., Yu, X., Hu, M., 2007. The conservative and non-conservative behavior of chromophoric dissolved organic matter in Chinese estuarine waters. Marine Chemistry 107, 357–366.
Hong, H., Wu, J., Shang, S., Hu, C., 2005. Absorption and fluorescence of chromophoric dissolved organic matter in the Pearl River Estuary, South China. Marine Chemistry 97, 78–89.
Hong, H., Zhang, C., Shang, S., Huang, B., Li, Y., Li, X., 2009. Interannual variability of summer coastal upwelling in the Taiwan Strait. Continental Shelf Research 29, 479–484.
Hu, C., Muller-Karger, F.E., Taylor, C., Carder, K.L., Kelble, C., Johns, E., Heil, C., 2005. Red tide detection and tracing using MODIS fluorescence data: a regional example in SW Florida coastal waters. Remote Sensing of Environment 97, 311–321.
Hu, C., Lee, Z., Muller-Karger, F.E., Carder, K.L., Walsh, J.J., 2006. Ocean color reveals phase shift between marine plants and yellow substance. IEEE Geoscience and Remote Sensing Letters 3, 262–266.
Jan, S., Wang, J., Chao, C.S., 2002. Seasonal variation of the circulation in the Taiwan Strait. Journal of Marine Systems 35, 249–268.
Jerlov, N.G., 1968. Optical Oceanography. Elsevier, Amsterdam, 194 pp.
Karentz, D., Lutze, L.H., 1990. Evaluation of biologically harmful ultraviolet radiation in Antarctica with a biological dosimeter designed for aquatic environments. Limnology and Oceanography 35, 549–561.

Lee, Z., Carder, K.L., Arnone, R.A., 2002. Deriving inherent optical properties from water color: a multiband quasi-analytical algorithm for optically deep waters. Applied Optics 41, 5755–5772.
Lee, Z., Carder, K.L., Arnone, R.A., 2009. Quasi-Analytical Algorithm (Version 5), on line, PDF file. http://www.ioccg.org/groups/Software_OCA/QAA_v5.pdf.
Lee, Z., 2005. A model for the diffuse attenuation coefficient of downwelling irradiance. Journal of Geophysical Research 110, C02016.
Mannino, A., Russ, M.E., Hooker, S.B., 2008. Algorithm development and validation for satellited-detrived distributions of DOC and CDOM in the U.S. Middle Atlantic Bight. Journal of Geophysical Research 113, C07051.
Mitchell, B.G., Bricaud, A., Carder, K., Cleveland, J., Ferrari, G.M., Gould, R., Kahru, M., Kishino, M., Maske, H., Moisan, T., Moore, L., Nelson, N., Phinney, D., Reynolds, R. A., Sosik, H., Stramski, D., Tassan, S., Trees, C., Weidemann, A., Wieland, J.D., Vodacek, A., 2000. Determination of Spectral Absorption Coefficients of Particles, Dissolved Material and Phytoplankton for Discrete Water Samples. Ocean Optics Protocols For Satellite Ocean Color Sensor Validation. NASA Technical Memorandum. 125–153.
O'Reilly, J.E., Maritorena, S., O'Brien, M.C., 2000. SeaWiFS Post-launch Calibration and Validation Analyses. NASA Technology Memorandum, pp. 49.
Parsons, T.R., Maita, Y., Lalli, C.M., 1984. A Manual of Chemical and Biological Methods for Seawater Analysis. Pargamon Press, Oxford, pp. 184.
Rochelle-Newall, E.J., Fisher, T.R., 2002. Chromophoric dissolved organic matter and dissolved organic carbon in Chesapeake Bay. Marine Chemistry 77, 23–41.
Siegel, D.A., Maritorena, S., Nelson, N.B., Hansell, D.A., Lorenzi-Kayser, M., 2002. Global distribution and dynamics of colored dissolved and detrital organic materials. Journal of Geophysical Research 107, 3228. doi:10.1029/2001JC000965.
Wang, Z., Chen, Q., 1989. On cold water intrusion in the Eastern Taiwan Strait during the cold season. Acta Oceanographica Taiwanica 22, 43–67 (in Chinese, with English Abstr).
Whitehead, K., Vernet, M., 2000. Influence of mycosporine-like amino acids (MAAs) on UV absorption by particulate and dissolved organic matter in La Jolla Bay. Limnology and Oceanography 45, 1788–1796.
Wu, B., 1982. Some problems on circulation study in Taiwan Strait. Journal of Oceanography in Taiwan Strait 1, 1–7 (in Chinese, with English Abstr).
Zeng, G., Hong, Q., 1980. Multi-year mean hydrological characteristics of Taiwan Strait and adjacent sea areas. Marine Science Bulletin 7 (in Chinese).
Zhang, Z., 2000. The analysis of hydrological characteristic of Min Jiang drainage area. Hydrology 20, 55–58 (in Chinese, with English Abstr).
Zhu, J., Li, T., 2003. The selection of the reference wavelength of spectra absorption curve of yellow substance. Ocean Technology 22, 11–41 (in Chinese, with English Abstr).